Gene Therapy
https://doi.org/10.1038/s41434-019-0109-0

ARTICLE

Inhibition of miR-296-5p protects the heart from cardiac hypertrophy by targeting CACNG6

Wei Wang[1] · Nian Liu[1] · Li Xin[1] · Yanfei Ruan[1] · Xin Du[1] · Rong Bai[1] · Jianzeng Dong[1] · ChangSheng Ma[1]

Received: 19 May 2019 / Revised: 23 September 2019 / Accepted: 16 October 2019

Abstract

Heart often undergoes mal-remodeling and hypertrophic growth in response to pathological stress. MiRNAs can regulate the cardiac function and participate in the regulation of cardiac hypertrophy. The present study aims at identifying the role of miR-296-5p in cardiac hypertrophy and further the underlying mechanism in hypertrophic cascades. Mice with cardiac hypertrophy were established by transverse aortic constriction (TAC). Cardiac hypertrophy in cardiomyocytes was induced by angiotensin II. Expression of miR-296-5p and its target gene CACNG6 was examined in cardiomyocytes transfected by miRNA. The expression of miR-296-5p was upregulated in mice with TAC surgery. The inhibition of miR-296-5p attenuated cardiac hypertrophy both in vitro and in vivo. And dual-luciferase reporter assays showed CACNG6 was the direct target of miR-296-5p, which modulated the expression of calcium signaling. MiR-296-5p was found to aggravate cardiac hypertrophy by targeting CACNG6, which suggests inhibition of miR-296-5p might have clinical potential to suppress cardiac hypertrophy and heart failure.

Introduction

Heart often undergoes mal-remodeling and hypertrophic growth in response to pathological stress [1]. Hypertrophy is a process which is characterized by the elevation of the size of cardiomyocyte with cell number unchanged [2]. Prolonged cardiac hypertrophy is one of the causes of heart failure and sudden death [3]. It was suggested that molecular events controlling heart development should be redeployed to control hypertrophic growth. Cardiac hypertrophy is always involved in the alteration of cardiac fetal genes such as brain natriuretic peptide (BNP), β myosin heavy chain (β-MHC) and others that encode atrial natriuretic peptide. Besides the upregulation of fetal genes, pathological hypertrophy is also associated with increased fibrosis, and reduction of cardiac dysfunction [4]. However, the molecular mechanism of cardiac hypertrophy is not fully understood.

MicroRNAs (miRNAs) are a class of small noncoding RNAs that can legate messenger RNAs (mRNAs) at partially complementary binding sites, and hence regulate the rate of protein synthesis by altering the stability of the targeted mRNAs [5]. They can negatively regulate posttranscriptional gene expression. Increasing evidences have demonstrated that miRNAs participate in the modulation of cell differentiation, apoptosis, development, and proliferation [6]. MiRNAs can regulate cardiac function including electric signals conduction, myocardial contraction, heart growth, and morphogenesis [7–9]. They can also participate in the regulation of cardiac hypertrophy. However, the roles of miRNAs in cardiac hypertrophy and remodeling are not yet clear.

Growing evidences have showed miR-212/132, miR-22, miR-208a, miR-27b, and miR-378 are involved in cardiac hypertrophy development. Genetic studies have revealed that miR-296-5p has been involved in the progression of glioblastoma, lung cancer, and other malignant tumors [10–12]. In cardiovascular disease, microarray analysis in the failing heart showed the upregulation of miR-296-5p at both 5 and 28 days in the failing hearts of mice [13].

Our research has previously detected the expression of miR-296-5p in cardiac hypertrophy. It was upregulated in mice with transverse aortic constriction (TAC) induced cardiac hypertrophy. Therefore, further investigation on function of miR-296-5p in cardiac hypertrophy is necessary for better understanding the regulation of cardiac homeostasis. In the present study, we aim to elucidate the role of miR-296-5p in cardiac hypertrophy, thus, it is necessary to

✉ ChangSheng Ma
tougao201801@sina.com

[1] Department of Cardiology, Beijing Anzhen Hospital, Capital Medical University, National Clinical Research Center for Cardiovascular Diseases, Beijing, China

identify the potential regulation of miR-296-5p in cardiac hypertrophy along with the underlying mechanism.

Materials and methods

Transverse aortic constriction

TAC procedure was performed on male C57BL/6 mice obtained from Beijing Vital River laboratory animal center. Sixty mice weighing 25–30 g (8 weeks) were anesthetized with isoflurane and subjected to thoracotomy. The aorta was dissected and tied with a 7–0 silk thread around the vessel using a 26-gauge needle to ensure consistent occlusion. Mice in sham group underwent thoracotomy and aortic dissection without constriction of the aorta. TAC was validated with significant increase in the ratio of heart weight-to-tibial length (HW/TL) and changes in echocardiography. Approximately 2% mice could not survive after the TAC surgery because of the bleeding complication. All the animal procedures were performed in accordance with the guidelines of Capital Medical University Animal Care and Use Committee.

Cardiomyocyte culture and transfections

Neonatal mouse cardiomyocytes were isolated from the heart of newborn C57BL6 mice (1–2 day old). After the thoracotomy, the heart popped out, and was quickly excised. The ventricles were isolated and transferred into cold Hank's balanced salt solution (HBSS) without Ca^{2+} and Mg^{2+} (Gibco, Invitrogen, Carlsbad, CA). The tissue was dispersed in a series of incubations at 37°C in HBSS containing 1.2 mg/ml pancreatin and 0.14 mg/ml collagenase. After centrifugation, cells were resuspended in Dulbecco's modified Eagle's medium (Gibco) containing 10% fetal bovine serum (Gibco) supplemented with antibiotics (penicillin, streptomycin; Gibco). Cells were cultured at 37 °C in humidified atmosphere of 95% air and 5% CO_2. For experiments, the cells were plated in a six-well plate at a density of 2×10^5 cells per well. After 24 h of culturing, the cells were transducted with ad-anti-miR-296-5p and ad-si-NC (GenePharma) at 2×10^5 viral particles/mL.12 h after transduction, the cultures were replaced with serum free medium for additional 48 h in the 1 μM angiotensin II (ang II, Sigma, USA).

Quantitative real-time PCR (qRT-PCR)

Total RNA from heart tissue or cardiomyocytes cultures was extracted according to the Trizol (Invitrogen) instructions. The concentration and purity of RNA were detected using the ultramicrospectrophotometer (NanoDrop, thermo, USA). For reverse transcription, the sample of RNA was reversely transcribed to cDNA, with a total system of 20 μl. Reverse transcription was performed at 25 °C for 5 min, 50 °C for 45 min, and followed by inactivation of the reverse transcriptase at 85 °C for 5 min. The cDNA was synthesized and analyzed by qRT-PCR, and the qRT-PCR was conducted referring to the instruction of SYBR® Premix Ex Taq™ II reagent kit (Takara, Dalian, China). The mRNA level of target genes was normalized to β-actin genes. The gene expression levels of ANP, BNP, and β-MHC in cardiomyocytes treated by angiotensin II were determined by real-time quantitative RT-PCR using $2^{-\Delta\Delta Ct}$ method. The mRNA expression of CACNG6 were also detected in cardiomyocytes transfected with ad-anti-miR-296-5p. The expression levels of mRNA were analyzed with six replicates from three independent experiments.

3′-UTR luciferase reporter assays

TargetScan was used to predict potential targets of miR-296-5p. The luciferase assays were then performed to further confirm the relationship of miR-296-5p and CACNG6 in cardiomyocytes. The vector for overexpression of CACNG6 3′-UTR was purchased from GenePharma. HEK293 cells were transfected with the full-length 3′-UTR of CACNG6 downstream of renilla luciferase gene in the presence of either miR-296-5p mimic or control miRNA mimic and co-transfected with a pGL3-Basic control plasmid (firefly luciferase) to generate pGL3-basic- CACNG6 3′-UTR-WT. A seed sequence transversion mutated version of the CACNG6 3′-UTR, named pGL3-basic- CACNG6 3′-UTRMut, was constructed as a control. Twenty-four hours after transfection, the cell lysates were collected and sequentially used for the detection of luciferase activity. The luciferase activity was measured with a Luciferase Reporter Assay System (Promega) and normalized to the activity of the Renilla luciferase gene.

Adenovirus application on TAC models

Mice were randomly divided into different groups. The transduction of ad-anti-miR-296-5p or ad-anti-NC was conducted in mice with injection in the heart 1 week before TAC operation (3.5×10^7 viral particles). Two skilled technicians were blind to the grouping and performed the injection. After 4 weeks, the hearts were collected and the left ventricle was rapidly frozen in liquid nitrogen and stored at −80 °C for subsequent experiments.

Echocardiography in mice

Echocardiography was performed using a Visualsonics Vevo 2100 (Visualsonics) ultrasound system with a 40-MHz

transducer. The left ventricular end-systolic diameter (LVESD) and left ventricular end-diastolic pressure (LVEDP) were measured. Percentage of left ventricular fractional shortening (LVFS) and left ventricular ejection fraction (LVEF) was calculated according to the System. The parameters were analyzed from at least three cardiac cycles. Data were collected from six mice in each group.

Immunostaining

Cells for immunostaining were fixed with 4% paraformaldehyde for 20 min and permeabilized with 0.5% Triton X-100 for 15 min, and then blocked with 3% BSA for 30 min. Cells were incubated with the indicated primary antibody (α-SMA, Abcam, Cambridge, England) at 4 °C overnight. After wash for three times, the blots were incubated with Alexa Fluor-labled secondary antibody (Invitrogen, CA, USA) for 2 h followed with DAPI staining for another 10 min (Olympus, Japan).

Histology assay

Heart samples from mice were collected at 4 weeks after TAC. The specimen were fixed with 4% paraformaldehyde and embedded in paraffin and cut into 5 μm in thickness sections and stained with hematoxylin & eosin following the instructions.

Western blot analysis

Samples were lysed in RIPA lysis buffer containing EDTA-free protease inhibitor cocktail (Roche) on ice for 30 min and centrifuged at 12,000 × g for 15 min at 4 °C. The supernatants were collected and stored at −80 °C. The protein concentrations were measured using the BCA Protein Assay Kit (Beyotime) according to the manufacturer's protocol. The tissue or cell extracts were subjected to SDS-PAGE and western blot analysis. Proteins blotted on PVDF membranes were incubated with the following primary antibodies overnight at 4 °C: CACNG6 (abcam; 1:1000, ab30966), p-PLN (abcam, 1:2000, ab15000), PLN (abcam, 1:2000, ab2865), RyR2 (abcam, 1:2000, ab2868), SERCA2 (abcam; 1:2000, ab2861), β-actin (Sigma, 1:1000, A3854). Donkey anti-mouse (1:5000) or goat anti-rabbit (1:5000) secondary antibodies (BBI life science D110085, D110058) were utilized. The protein bands were visualized using the chemiluminescence Imaging System (Tannon). Blots were analyzed from three biological replicates.

Statistical analysis

All data are presented as the mean ± standard deviation (SD) for at least three repeated individual experiments and were analyzed using GraphPad Prism™, version 5.00 software (GraphPad, La Jolla, CA, USA). Statistical significance was then determined with an unpaired two-tailed Student's *t* test (for two groups). A value of $P < 0.05$ was considered statistically significant.

Results

Upregulation of miR-296-5p were identified in the myocardium from mice undergoing TAC

This phenomenon was also confirmed in cardiomyocytes treated with angiotensin II. It displayed larger size in cardiomyocytes with ang II treatment than normal cells (Fig. 1a). The levels of ANP, BNP, and β-MHC are always used to evaluate the extent of myocardial hypertrophy, Their level in the Ang II treatment group were identified to be elevated (Fig. 1b). The HE staining revealed a significant larger size in the TAC treated heart than that in sham group (Fig. 1c). Moreover, echocardiographic parameters of the mice including LVEDP, LVFS, LVEF, LVESD were evaluated with an ultrasound system, which further indicated that the cardiac function of the mice subjected to TAC was impaired (Fig. 1d, e). In order to detect the expression level of miR-296-5p in cardiac tissues of mice with cardiac hypertrophy, we measured their levels using TaqMan quantitative PCR in the tissues from left ventricles of mice with cardiac hypertrophy and sham. MiR-296-5p expression was upregulated in myocardium with cardiac hypertrophy compared with sham which is in consistence with the ratio of HW/TL (Fig. 1f, g). Similarly, the miR-296-5p expression was upregulated in cardiomyocytes with ang II treatment than normal cells (Fig. 1h).

Inhibition of miR-296-5p suppressed cardiac hypertrophy both in vitro and in vivo

To identify whether inhibition of miR-296-5p protects cardiomyocytes from stimuli-induced hypertrophy, cardiomyocytes were transducted with adenovirus vector containing anti-miR-296-5p. To detect the efficient of the adenovirus, we evaluate the expression of miR-296-5p in each group and the results indicated that adenovirus of anti-miR-296-5p significantly downregulated the expression of miR-296-5p both in vivo and in vitro in comparison with that in anti-NC group (Fig. 2a, b). In response to Ang II, the average cardiomyocytes size was decreased in anti-miR-296-5p group compare with anti-NC group, suggesting that inhibition of miR-296-5p restored cardiomyocyte phenotype under stimulation of Ang II (Fig. 2d). Moreover, inhibition of miRNA-296-5p significantly reduced the

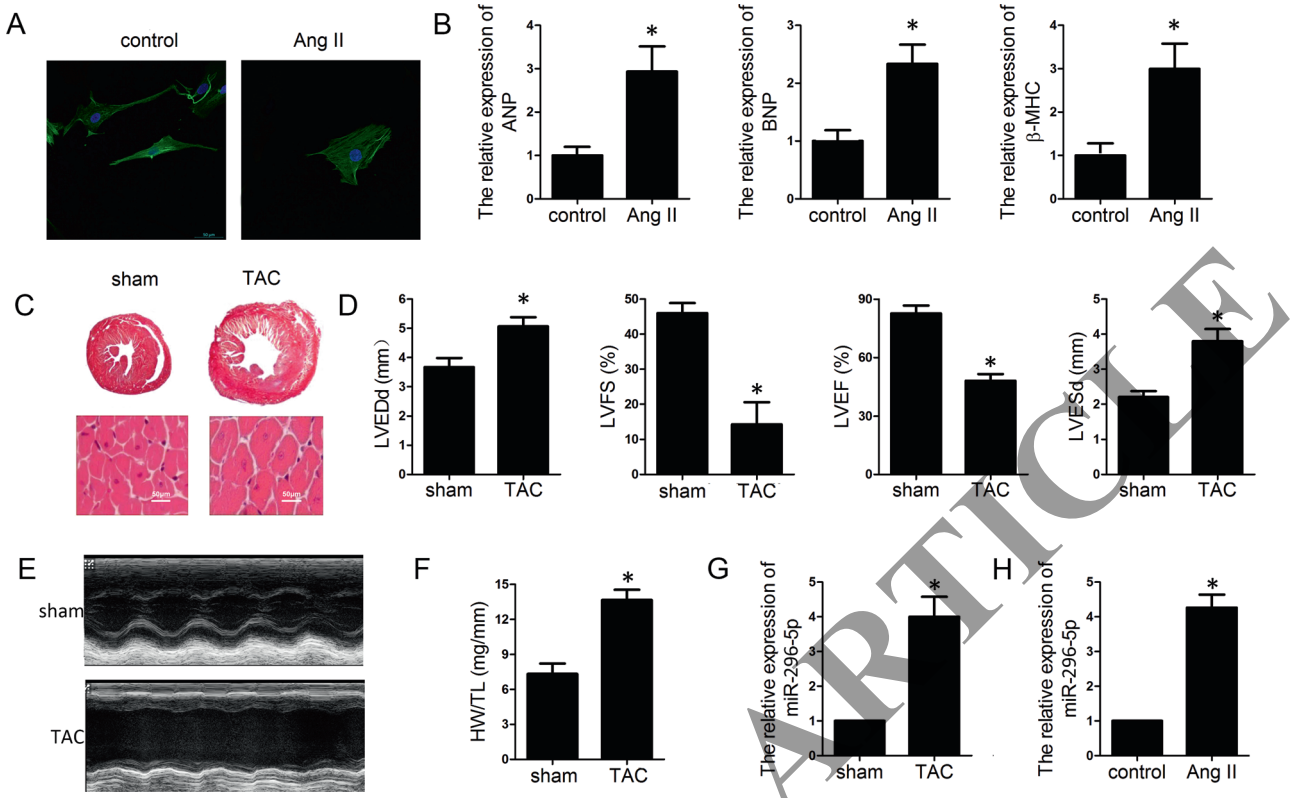

Fig. 1 MiR-296-5p was upregulated in cardiomyocytes and myocardium subjected to Ang II and TAC treatment, respectively. **a** Immunostaining of α-SMA was used to evaluate the size of cardiomyocyte subjected to Ang II treatment or not. **b** The levels of myocardial hypertrophy biomarker ANP, BNP, and β-MHC are detected using qPCR. **c** Hematoxylin and eosin staining of the heart under sham and TAC treatment. **d**, **e** Echocardiographic parameters of the mice including LVEDP, LVFS, LVEF, LVESD were evaluated with an ultrasound system. **f** Quantification of heart weight-to-tibial length ratio. **g**, **h** The expression of miR-296-5p was detected with qPCR. $*p < 0.05$ vs control or sham group.

expression level of ANP, BNP, and β-MHC compared with that in anti-NC group (Fig. 2g) in consistence with the ratio of HW/TL (Fig. 2h).

To elucidate whether inhibition of miR-296-5p could decrease cardiac hypertrophy in vivo, mice were injected with ad-anti-miR-296-5p in the heart 1 week after the TAC surgery. TAC-induced cardiac hypertrophy in mice was expected to be reflected by increased heart weight, and ad-anti-miR-296-5p treatment in mice reversed these TAC-induced changes. Cardiomyocytes size as determined in histological sections of hearts was significantly decreased in ad-anti-miR-296-5p group compared with ad-anti-NC group (Fig. 2c). For the cardiac function, parameters including LVEDP, LVFS, LVEF, LVESD were detected. LVEDP and LVESD were significantly reduced in ad-anti-miR-296-5p group compared with the ad-anti-NC. LVFS and LVEF were significantly improved in ad-anti-miR-296-5p group at 4 weeks (Fig. 2f). Taken together, these results demonstrated that the inhibition of miR-296-5p could protect heart from cardiac hypertrophy both in vitro and in vivo.

MiR-296-5p inhibited CACNG6 expression by binding to its 3′-UTR

To explore the further mechanism of miR-296-5p in cardiac hypertrophy, we investigated the potential target genes of miR-296-5p using bioinformatics scan. We found that the 3′-UTR of the CACNG6 gene contains a highly conserved miR-296-5p seed sequence, suggesting that CACNG6 was a target for miR-296-5p (Fig. 3a). To validate the prediction, we detected the possible miR-296-5p seed sequence in the 3′-UTR of CACNG6 using the TargetScan algorithms and cloned the 3′-UTR of wild-type and mutant CACNG6 into the luciferase reporter gene system. The activity of the luciferase reporter gene linked to the 3′-UTR of wild-type CACNG6 was reduced with the presence of miR-296-5p, while that of mutant CACNG6 did not change (Fig. 3b). To further confirm the correlation between miR-296-5p and CACNG6, we validated the expression of CACNG6 in cardiomyocytes. The results showed the protein expression of CACNG6 was obviously decreased in cardiomyocytes with ad-miR-296-5p infection (Fig. 3c, d). Moreover, we detected

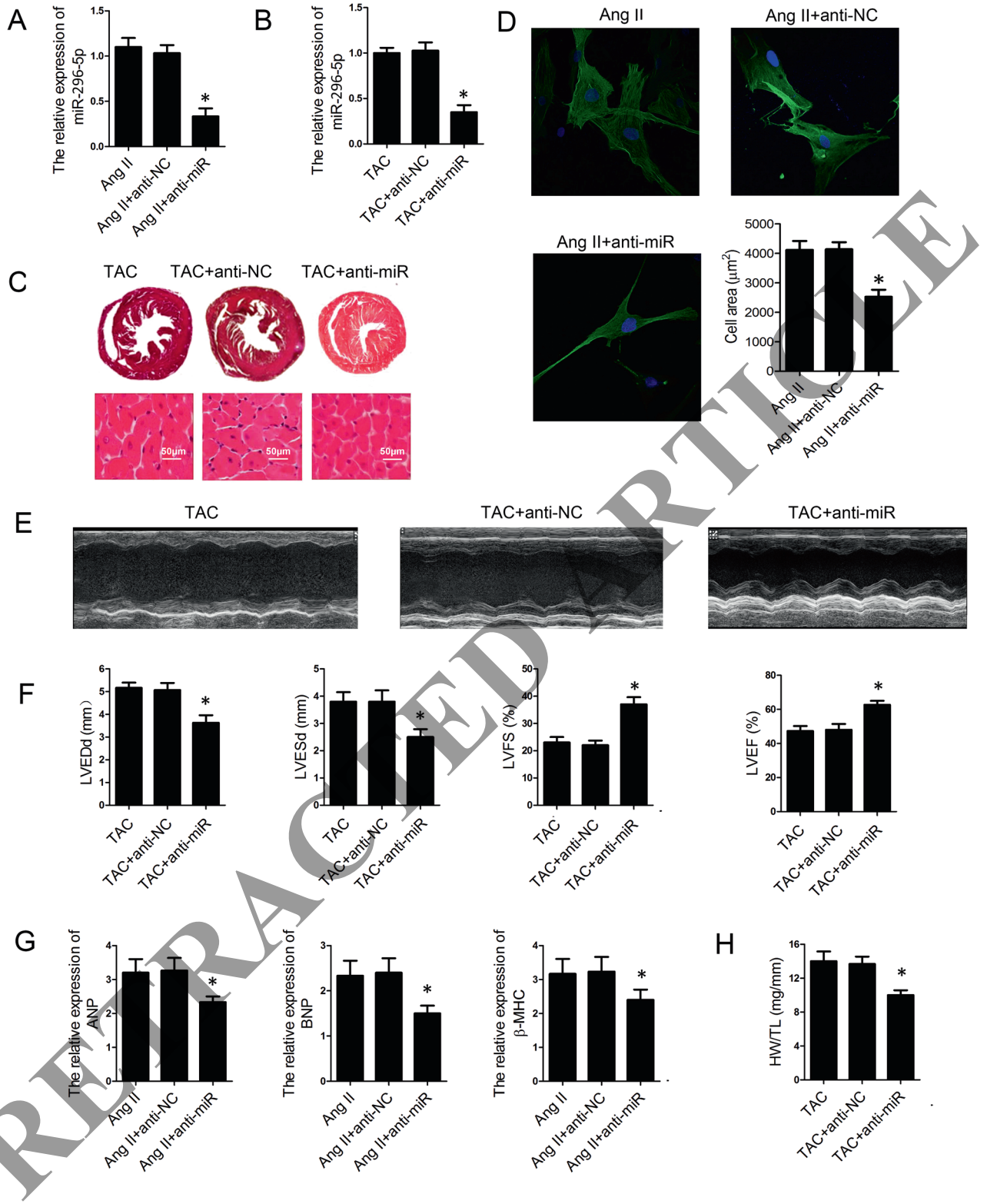

Fig. 2 MiR-296-5p knockdown released the hypertrophy induced by Ang II and TAC treatment. a, **b** MiR-296-5p was downregulated in cardiomyocyte and myocardium subjected to ad-anti-miR-295-5p infection respectively. **c** Hematoxylin and eosin staining of the heart under TAC, TAC + anti-NC and TAC + anti-miR-296-5p treatment. **d** Immunostaining of α-SMA was used to evaluate the size of cardiomyocyte subjected to Ang II, Ang II + anti-NC and Ang II + anti-miR-296-5p treatment respectively. **e**, **f** Echocardiographic parameters of the mice including LVEDP, LVFS, LVEF, LVESD were evaluated with a ultrasound system. **g** The level of myocardial hypertrophy biomarker ANP, BNP, and β-MHC are detected using qPCR. **h** Quantification of heart weight-to-tibial length ratio. *$p < 0.05$ vs Ang II + anti-NC group or TAC + anti-NC group.

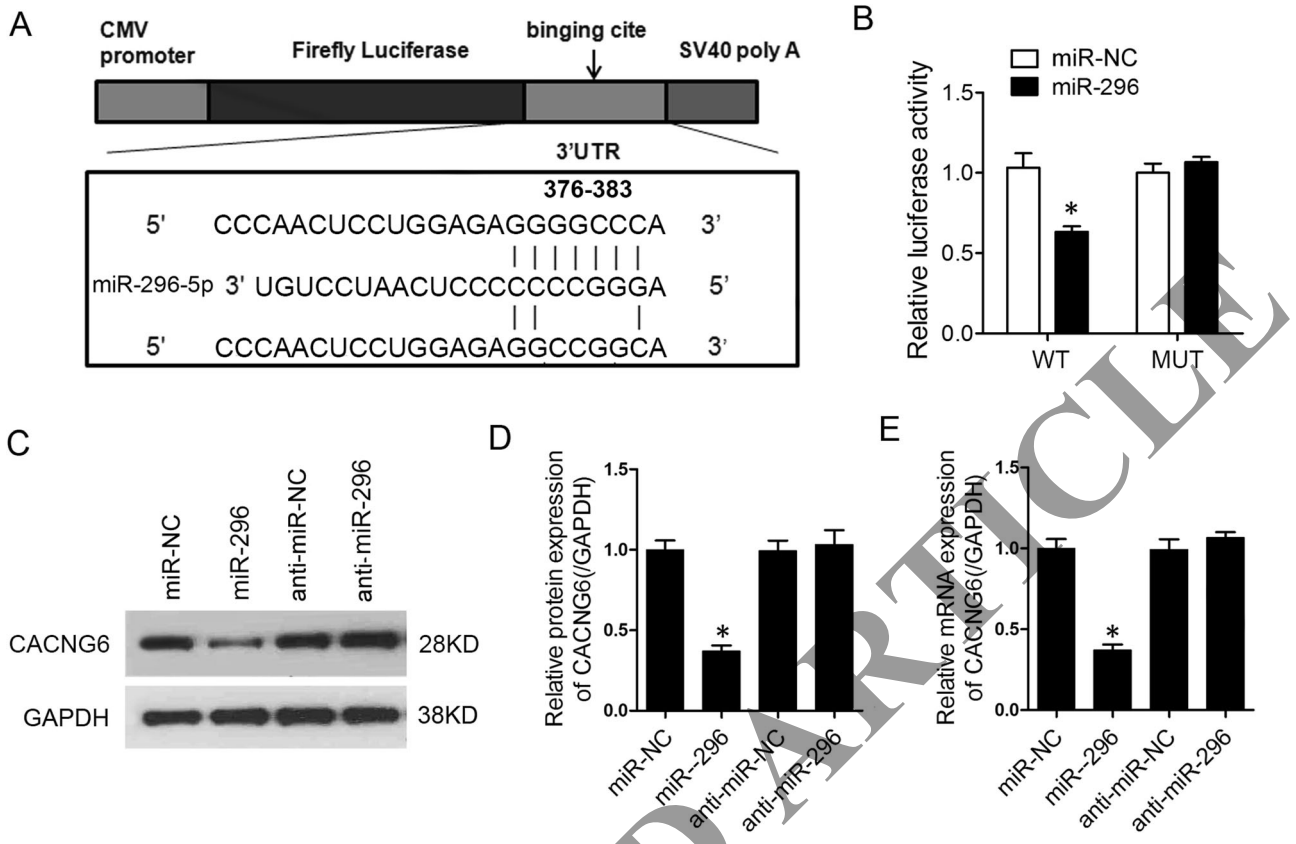

Fig. 3 MiR-296-5p directly targets CACNG6 in the mouse cardiomyocytes. a The binding of miR-296-5p sites in the 3′-UTR of CACNG6 are shown. **b** Luciferase activity assay was performed to identify whether CACNG6 was the direct target gene of miR-296-5p. **c**, **d** Western blot was used to evaluate the protein expression under infection of ad-miR-296-5p and ad-anti-miR-296-5p. **e** qPCR was used to evaluate the RNA expression under infection of ad-miR-296-5p and ad-anti-miR-296-5p. $*p < 0.05$ vs miR-NC group.

the mRNA level of CACNG6 and found that mRNA expression of CACNG6 was decreased in cardiomyocytes with ad-miR-296-5p infection (Fig. 3e). Together, these data indicated that CACNG6 was the direct target of miR-296-5p.

Overexpression of CACNG6 reversed the repression of cardiac hypertrophy

We further evaluated the role of CACNG6 in cardiac hypertrophy by gain of function experiments. Overexpression of CACNG6 with the infection of ad-CACNG6 was performed in cardiomyocytes to determine its role in cardiac hypertrophy. QPCR assay was used to evaluate the CACNG6 expression. The results indicated a significant elevated level of CACNG6 in cardiomyocyte and myocardium after infection with ad-CACNG6 (Fig. 4a, b). Consistent with the effect of miR-296-5p knockdown in cardiomyocytes, overexpression of CACNG6 partially rescued cardiac hypertrophic growth. Assessment of cardiomyocyte size and the expression of hypertrophic genes including ANP, BNP, and β-MHC demonstrated that the overexpression of CACNG6 repressed cardiac hypertrophy induced by Ang II treatment (Fig. 4c–e). In addition, HE staining indicated that overexpression of CACNG6 exhibited the attenuation of cardiac hypertrophy in mice (Fig. 4f). Furthermore, LVEDP and LVESD were significantly reduced in ad-CACNG6 group compared with control group. LVFS and LVEF were significantly improved in ad-CACNG6 group in comparison with that in control group (Fig. 4g, h).

Inhibition of miR-296-5p protected heart from cardiac hypertrophy via CaMKII regulation pathway

Research has shown that CACNG6 participates in the modulating of voltage-dependent calcium channels, and CaMKII regulation was confirmed to play an important role in cardiac hypertrophy. To investigate whether the inhibition of miR-296-5p improves heart function via modulating CaMKII signaling in cardiomyocytes, CaMKII, SERCA2, and CaMKII-dependent PLN were assessed by western blotting. After infection of ad-anti-miR-296-5p, the expression of CACNG6 was reversely restored. Next, with the treatment of ad-anti-miR-296-5p, the expression of

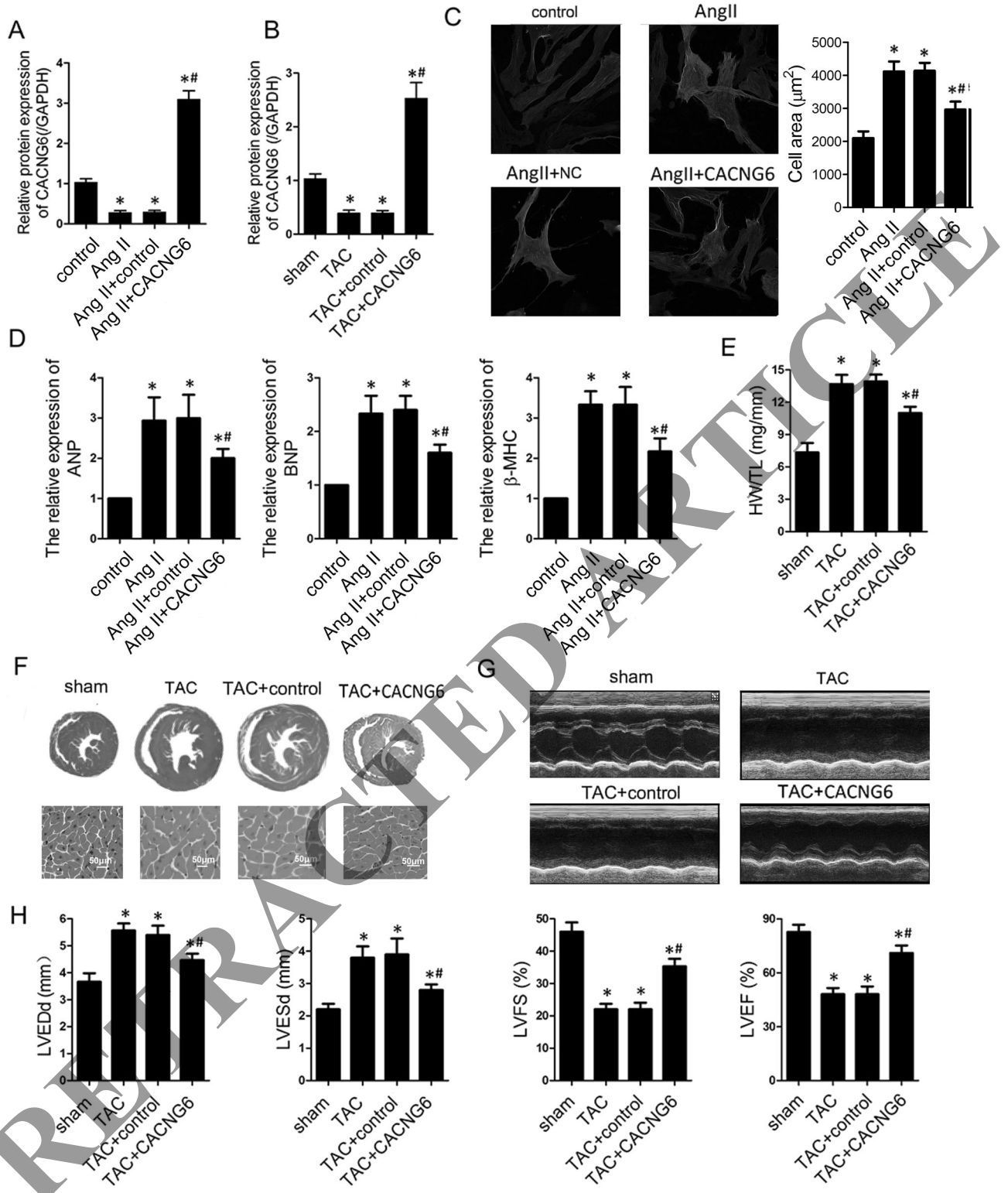

Fig. 4 CACNG6 overexpression released the hypertrophy induced by Ang II and TAC treatment. a, **b** CACNG6 overexpression was upregulated in cardiomyocyte and myocardium subjected to ad-CACNG6 infection respectively. **c** Immunostaining of α-SMA was used to evaluate the size of cardiomyocyte subjected to Ang II, Ang II + CACNG6 treatment. **d** The level of myocardial hypertrophy biomarkers ANP, BNP, and β-MHC are detected using qPCR. **e** Quantification of heart weight-to-tibial length ratio. **f** Hematoxylin and eosin staining of the heart under TAC, TAC + an-CACNG6 treatment. **g**, **h** Echocardiographic parameters of the mice including LVEDP, LVFS, LVEF, LVESD were evaluated with a ultrasound system. $^{*}p < 0.05$ vs Ang II or TAC group, $^{\#}p < 0.05$ vs Ang II + control or TAC + control group.

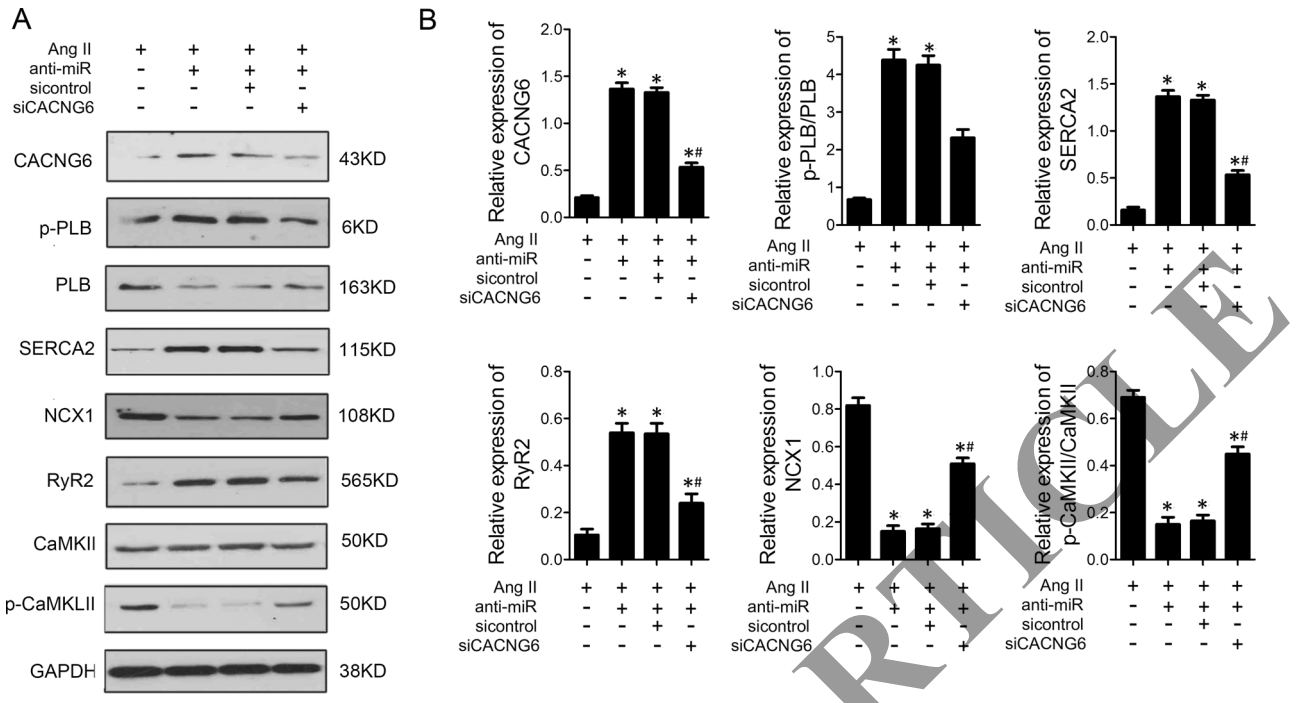

Fig. 5 MiR-296-5p knock downregulated expression of the CACNG6 relative proteins. a, b Western blot assay was carried out to evaluate the expression level of p-PBL, PBL, SERCA2, NCX1, RyR2, CaMKII, p-CaMKII. $^{*}p < 0.05$ vs Ang II group, $^{\#}p < 0.05$ vs Ang II + anti-miR + sicontrol group.

p-PLB, RyR2, and SERCA2 was upregulated, while the expression of PLB and p-CaMKII was reversely downregulated. Excessive CaMKII activity contributes to cardiac hypertrophy, thus, these data identified that the inhibition of miR-296-5p could attenuate cardiac hypertrophy by increasing the expression of CACNG6 and modulating CaMKII signaling (Fig. 5a, b).

Deletion of CACNG6 reversed the effect of miR-296-5p knockdown in cardiomyocyte

In order to further investigate the relation between CACNG6 and miR-296-5p. We performed rescue experiment. SiRNA of CACNG6 was used to knockdown CACNG6 level which was confirmed to be useful by the qPCR results (Fig. 6a). Thereafter, we evaluate the cell area of cardiomyocytes. As Fig. 6b, c revealed, siCACNG6 reversed the effect of miR-296-5p deletion. Subsequently, expression level of ANP, BNP, and β-MHC was detected. We found that siCACNG6 reversed the function of miR-296-5p knockdown on the level of ANP, BNP, and β-MHC (Fig. 6d).

Discussion

Amplification of the 20q13.32 genomic region has been found in various cancers types [14–16]. miR-296 has been categorized as an Angio-miR, along with miR-378 and miR-17-92 in the same gene cluster, due to its contribution to tumor angiogenesis [17, 18].

MiR-296 was upregulated in normal human brain endothelial cells in response to exposure to human brain glioma cells. Down-and upregulation of miR-296 resulted in the inhibition and induction, respectively, of morphologic characteristics associated with angiogenesis of human endothelial cells [18]. Downregulation of miR-296 was shown to inhibit esophageal cancer cell progression by regulation of multiple signaling pathways including cyclin D1, p27, P-glycoprotein, Bcl-2, MDR1, and Bax [19]. MiR-296 also plays a critical role in the progression of gastric cancer, lung adenocarcinoma, and esophageal cancers [20]. As in the cardiovascular system, miR-269-5p was indicated to be upregulated in hypertrophic cardiomyopathy patients. This finding caught our attention on the role of miR-269-5p in the progression of cardiac hypertrophy [21].

In the present study, we found an altered expression level of miR-296-5p. The further in vivo and in vitro study demonstrated that inhibition of miR-296-5p significantly suppressed cardiac hypertrophy. Moreover, miR-296-5p depletion alleviated the damage of cardiac function induced by TAC.

miRNAs regulate the expression level of specific genes through combining to the targeting regions. We predicted the potential target gene of miR-296-5p using the bioinformatics

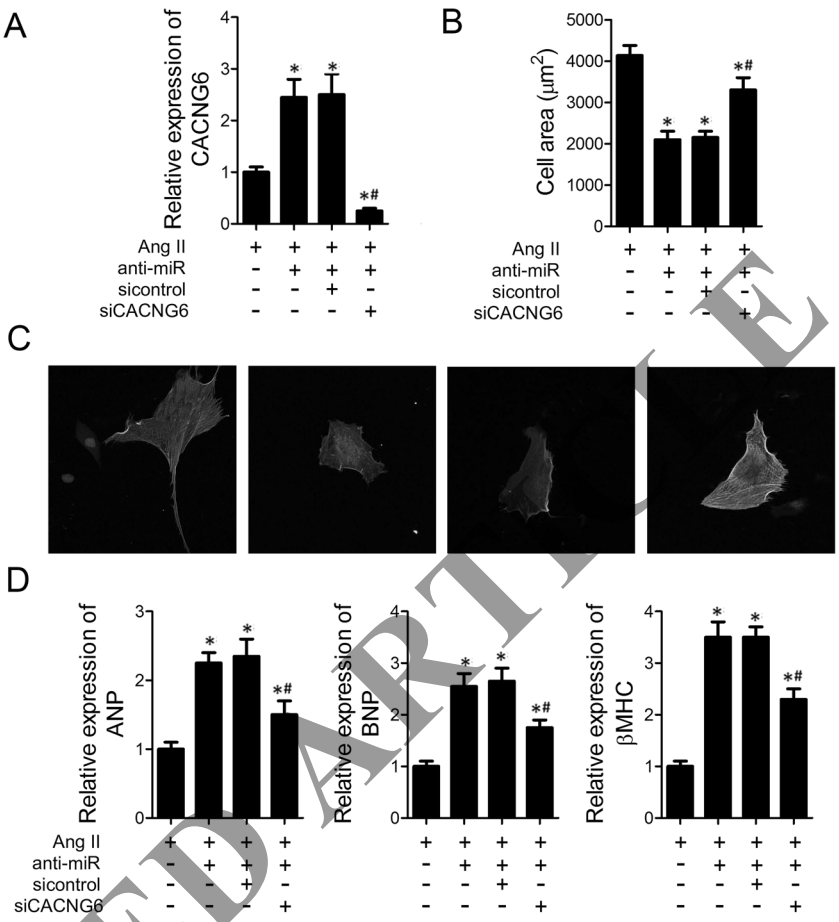

Fig. 6 Deletion of CACNG6 reversed the effect of miR-296-5p knockdown in cardiomyocyte. a QPCR was performed to evaluate the expression level of CACNG6. **b**, **c** Immunostaining of α-SMA was used to evaluate the size of cardiomyocyte subjected to Ang II treatment or not. **d** The level of myocardial hypertrophy biomarkers ANP, BNP, and β-MHC are detected using qPCR. $^{*}p < 0.05$ vs Ang II group, $^{\#}p < 0.05$ vs Ang II + anti-miR + sicontrol group.

analysis software. CACNG6 was confirmed to be a direct target of miR-296-5p in cardiomyocyte.

The calcium channel, voltage-dependent, gamma subunit 6 (CACNG6) gene encodes a protein that stabilizes the calcium channel [22]. Recent studies have revealed negative relations of CACNG6 gene expression to chronic obstructive pulmonary disease, responses of the human airway epithelium following injury and parenchyma in lung tissues [23]. The CACNG6 is an integral membrane protein that stabilizes the calcium channel during its inactive state [24]. Calcium channel function has been implicated in multiple cardiovascular diseases, such as hypertension and cardiac hypertrophy [25]. We subsequently evaluated the expression level of several calcium channel proteins. The results indicated that CACNG6 participates in the regulation of SERCA2, NCX1, RyR2, and the phosphorylation of PLB and CAMKLII. However, the downstream underlying mechanism are still unclear which need to been explored further.

Conclusions

MiR-296-5p was found to aggravate cardiac hypertrophy by targeting CACNG6, which suggested inhibition of miR-296-5p might have clinical potential to suppress cardiac hypertrophy and heart failure. In the present study, we first explored the effect of miR-296-5p in hypertrophy. In addition, we investigated the role of CACNG6 which is the direct target gene of miR-296-5p. Our findings suggested novel biomarkers or potential therapy targets of hypertrophy. Meantime, more further study should be listed in schedule.

Data availability

All data generated or analysed during this study are included in this published article.

Funding This work was supported by a grant from the National Science Foundation of China (81470430).

Author contributions WW and NL participated in the whole experiment and wrote the manuscript. LX helped interpret the data. YR did the animal experiment. XD and RB helped the acquisition of echocardiography data. CSM and JD designed and supervised the project.

Compliance with ethical standards

Conflict of interest The authors declare that they have no conflict of interest.

Ethics approval All the animal procedures were performed in accordance with the guidelines of Capital Medical University Animal Care and Use Committee.

Publisher's note Springer Nature remains neutral with regard to jurisdictional claims in published maps and institutional affiliations.

References

1. Nakamura M, Sadoshima J. Mechanisms of physiological and pathological cardiac hypertrophy. Nat Rev Cardiol. 2018;15:387–407.
2. Treibel TA, Kozor R, Menacho K, Castelletti S, Bulluck H, Rosmini S, et al. Left ventricular hypertrophy revisited: cell and matrix expansion have disease-specific relationships. Circulation. 2017;136:2519–21.
3. Aubdool AA, Argunhan F, Thakore P, Brain SD. Response by Aubdool et al. to letters regarding article, "A novel alpha-calcitonin gene-related peptide analogue protects against end-organ damage in experimental hypertension, cardiac hypertrophy, and heart failure". Circulation. 2018;137:1201–2.
4. Chatterjee S, Bar C, Thum T. Linc-ing the noncoding genome to heart function: beating hypertrophy. Trends Mol Med. 2017;23:577–9.
5. Ambros V. MicroRNA pathways in flies and worms: growth, death, fat, stress, and timing. Cell. 2003;113:673–6.
6. Yates LA, Norbury CJ, Gilbert RJ. The long and short of microRNA. Cell. 2013;153:516–9.
7. Cordes KR, Srivastava D. MicroRNA regulation of cardiovascular development. Circ Res. 2009;104:724–32.
8. Harada M, Luo X, Murohara T, Yang B, Dobrev D, Nattel S. MicroRNA regulation and cardiac calcium signaling: role in cardiac disease and therapeutic potential. Circ Res. 2014;114:689–705.
9. van Rooij E, Marshall WS, Olson EN. Toward microRNA-based therapeutics for heart disease: the sense in antisense. Circ Res. 2008;103:919–28.
10. Lopez-Bertoni H, Kozielski KL, Rui Y, Lal B, Vaughan H, Wilson DR, et al. Bioreducible polymeric nanoparticles containing multiplexed cancer stem cell regulating mirnas inhibit glioblastoma growth and prolong survival. Nano Lett. 2018;18:4086–94.
11. Lee H, Shin CH, Kim HR, Choi KH, Kim HH. MicroRNA-296-5p promotes invasiveness through downregulation of nerve growth factor receptor and caspase-8. Mol Cells. 2017;40:254–61.
12. Maia D, de Carvalho AC, Horst MA, Carvalho AL, Scapulatempo-Neto C, Vettore AL. Expression of miR-296-5p as predictive marker for radiotherapy resistance in early-stage laryngeal carcinoma. J Transl Med. 2015;13:262.
13. Muthusamy S, DeMartino AM, Watson LJ, Brittian KR, Zafir A, Dassanayaka S, et al. MicroRNA-539 is up-regulated in failing heart, and suppresses O-GlcNAcase expression. J Biol Chem. 2014;289:29665–76.
14. Nishimura T. Total number of genome alterations in sporadic gastrointestinal cancer inferred from pooled analyses in the literature. Tumour Biol. 2008;29:343–50.
15. Staaf J, Jonsson G, Ringner M, Vallon-Christersson J, Grabau D, Arason A, et al. High-resolution genomic and expression analyses of copy number alterations in HER2-amplified breast cancer. Breast Cancer Res. 2010;12:R25.
16. Uchida M, Tsukamoto Y, Uchida T, Ishikawa Y, Nagai T, Hijiya N, et al. Genomic profiling of gastric carcinoma in situ and adenomas by array-based comparative genomic hybridization. J Pathol. 2010;221:96–105.
17. Yoon AR, Gao R, Kaul Z, Choi IK, Ryu J, Noble JR, et al. MicroRNA-296 is enriched in cancer cells and downregulates p21WAF1 mRNA expression via interaction with its 3′ untranslated region. Nucleic Acids Res. 2011;39:8078–91.
18. Wurdinger T, Tannous BA, Saydam O, Skog J, Grau S, Soutschek J, et al. miR-296 regulates growth factor receptor overexpression in angiogenic endothelial cells. Cancer Cell. 2008;14:382–93.
19. Hong L, Han Y, Zhang H, Li M, Gong T, Sun L, et al. The prognostic and chemotherapeutic value of miR-296 in esophageal squamous cell carcinoma. Ann Surg. 2010;251:1056–63.
20. Fu Q, Song X, Liu Z, Deng X, Luo R, Ge C, et al. miRomics and proteomics reveal a miR-296-3p/PRKCA/FAK/Ras/c-Myc feedback loop modulated by HDGF/DDX5/beta-catenin complex in lung adenocarcinoma. Clin Cancer Res. 2017;23:6336–50.
21. Fang L, Ellims AH, Moore XL, White DA, Taylor AJ, Chin-Dusting J, et al. Circulating microRNAs as biomarkers for diffuse myocardial fibrosis in patients with hypertrophic cardiomyopathy. J Transl Med. 2015;13:314.
22. Jin L, Mao K, Li J, Huang W, Che T, Fu Y, et al. Genome-wide profiling of gene expression and DNA methylation provides insight into low-altitude acclimation in Tibetan pigs. Gene. 2018;642:522–32.
23. Cao Y, Li R, Li Y, Zhang T, Wu N, Zhang J, et al. Identification of transcription factor-gene regulatory network in acute myocardial infarction. Heart Lung Circ. 2017;26:343–53.
24. Burgess DL, Gefrides LA, Foreman PJ, Noebels JL. A cluster of three novel Ca2+ channel gamma subunit genes on chromosome 19q13.4: evolution and expression profile of the gamma subunit gene family. Genomics. 2001;71:339–50.
25. Westenbrink BD, Ling H, Divakaruni AS, Gray CB, Zambon AC, Dalton ND, et al. Mitochondrial reprogramming induced by CaMKIIdelta mediates hypertrophy decompensation. Circ Res. 2015;116:e28–e39.